JOURNAL OF AIRCRAFT
Vol. 46, No. 3, May–June 2009

Engineering Notes

ENGINEERING NOTES are short manuscripts describing new developments or important results of a preliminary nature. These Notes should not exceed 2500 words (where a figure or table counts as 200 words). Following informal review by the Editors, they may be published within a few months of the date of receipt. Style requirements are the same as for regular contributions (see inside back cover).

Assessment of Uncertain External Store Aerodynamics Using μ-p Flutter Analysis

Sebastian Heinze,* Ulf Ringertz,† and Dan Borglund‡
Royal Institute of Technology, 100 44 Stockholm, Sweden

DOI: 10.2514/1.39158

Nomenclature

c_p = pressure coefficient
D = uncertainty set
F = flutter matrix
f = frequency
g = nondimensional damping
K = stiffness matrix
k = reduced frequency
L = reference length
M = mass matrix
p = eigenvalue
Q = aerodynamic matrix
V = airspeed
w = uncertainty bound
δ = uncertainty parameter
η = modal coordinates
μ = structured singular value
ρ = air density
σ = damping
ω = circular frequency

Introduction

FLUTTER testing is rarely performed on full-scale aircraft, due to the high risk for structural damage and failure. Instead, flutter boundaries are computed based on a numerical model of the aircraft, and flight testing under less critical conditions can be performed to collect data for validation of the numerical model. Clearly, problems arise when the flight-test data show deviation from the numerically predicted data. Deviations are likely to occur for any aircraft configuration, because model imperfections and simplifications always lead to some uncertainty in the numerical model, and the question arises as to the impact that these uncertainties have on the predicted flutter boundaries.

In most cases, some parts of the numerical model, such as the mass properties of different components, are well known, whereas other elements, such as the aerodynamic loads in some region of a wing with complex geometry, are known to be subject to uncertainty. Earlier studies [1–3] have shown how aerodynamic uncertainties can be introduced in the numerical model based on physical reasoning and known modeling difficulties. The same technique for modeling of aerodynamic uncertainty will be applied in this study, but it will also be shown how data points collected at subcritical conditions can be used to establish an uncertainty model that is capable of producing reliable flutter boundaries.

In the present study, a wind-tunnel model was specifically designed to demonstrate and evaluate uncertainty modeling approaches. A fairly simple wing geometry and structure is chosen to minimize the errors introduced by modeling simplifications. An external store in the form of a wing-tip missile is used to increase the model complexity gradually, and the impact on the flutter behavior is investigated both numerically and experimentally. In cases in which the numerical predictions deviate from the experimental results, an uncertainty description is developed and μ-p flutter analysis and model validation [4] are applied to compute bounds on the flutter speed.

Experimental Setup

The considered model is a generic delta-wing configuration, as shown in Fig. 1a, with a semispan of 0.88 m and a mean chord of 0.70 m. The wing is mounted vertically on the floor in the low-speed wind tunnel L2000 at the Royal Institute of Technology. Because of the high risk involved in flutter testing, it was found convenient to design a low-cost wind-tunnel model with a low level of complexity. The wing consists of a glass-fiber plate with carbon-fiber stiffeners to obtain the desired structural properties. The wing can easily be equipped with external stores, such as an underwing missile and a wing-tip missile. In the present study, the impact of a wing-tip store will be investigated.

Structural Design

The wind-tunnel model is meant to represent a generic delta-wing configuration of a fighter aircraft. Because of the length and velocity scales imposed by the wind-tunnel environment, some properties such as the Mach number of the model will not represent the full-scale model. The model was, however, scaled in terms of the structural properties with respect to the aeroelastic behavior. The objective was to obtain eigenfrequencies f such that the reduced frequencies $k = 2\pi f \cdot L/V$ are the same for both model and full-scale aircraft, where L is a reference length (taken here as the mean semichord), and the velocity V is chosen at a typical flight condition.

In the present case, it was found that both the length-scaling and the velocity-scaling factors between model and full-scale aircraft are on the order of 10, making the frequency-scaling factor equal to one. Therefore, structural eigenfrequencies of the model were chosen to be equal to the eigenfrequencies of a representative full-scale structure. Because flutter behavior is typically governed by the most fundamental modes of a structure, the first bending and the first torsional eigenfrequencies were emphasized.

Received 17 June 2008; revision received 10 February 2009; accepted for publication 12 February 2009.

*Ph.D. Student, Department of Aeronautical and Vehicle Engineering, Division of Flight Dynamics, Teknikringen 8. Member AIAA.
†Professor, Department of Aeronautical and Vehicle Engineering, Division of Flight Dynamics, Teknikringen 8. Member AIAA.
‡Research Associate, Department of Aeronautical and Vehicle Engineering, Division of Flight Dynamics, Teknikringen 8. Member AIAA.

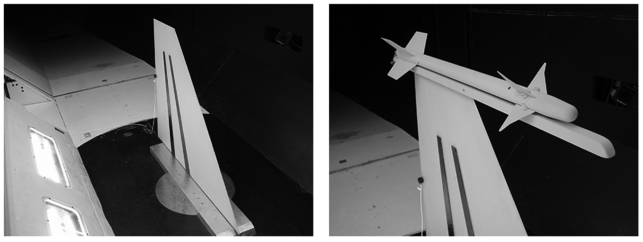

a) b)

Fig. 1 Photographs of a) delta wing in the wind tunnel and b) wing-tip external store.

To obtain specific eigenfrequencies as determined by the aeroelastic scaling, a few design parameters were defined in the structural design. In general, both eigenfrequencies and eigenmode shapes can be controlled by the mass and stiffness distribution. In the present study, a fixed-wing geometry was assumed, and a glass-fiber-composite plate was considered as a baseline structure. Carbon-fiber-composite spars were attached to the composite plate to control the structural properties of the wing. Two spars were mounted on both the upper and lower sides of the wing, and the spar dimensions and positions were chosen to obtain the desired eigenfrequencies. The mode shapes were not designed specifically.

External Store

The main focus of the study is to investigate the aerodynamic impact of an external store on the flutter behavior. A realistic wing-tip missile was therefore manufactured and mounted to the wing tip, as shown in Fig. 1b. The missile is mounted to a launcher beam that is assumed to be rigidly connected to the wing tip. Different configurations were considered to identify the aerodynamic impact of different missile components on the flutter behavior of the wing. Figure 2 shows the five considered configurations. To reduce the effects on the flutter speed due to structural differences between the different configurations, mass balancing was used to compensate for different components after they were removed from the wind-tunnel model. The mass balancing for the fins was located within the missile body, whereas the mass balancing for the missile was located within the launcher beam to maintain the aerodynamic shape of the wing-tip region.

Numerical Model

Numerical models of the delta wing were generated in both NASTRAN [5] and ZAERO [6]. The model is composed of shell elements for the wing, mass elements for the missile, and aerodynamic panels for both wing and missile. The missile assembly was assumed to be rigid.

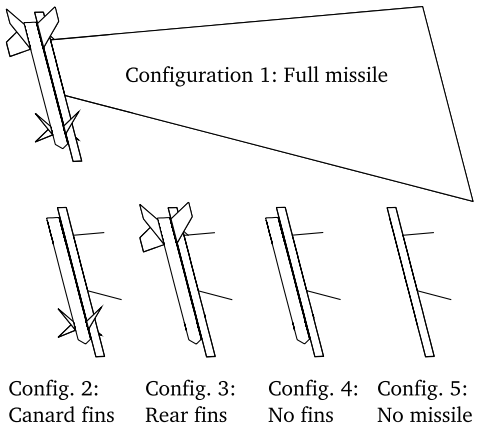

Fig. 2 Different configurations of the wing-tip external store.

Structural Modeling

The geometry of the structural elements of the wing plate was defined such that the location of the carbon-fiber spars coincides with the location of structural grid points to allow for accurate modeling of the different material properties. NASTRAN `CQUADR` elements were selected for connecting the structural grid points of the wing plate. Figure 3a shows the discretization of the structural elements of the wing plate. Note that the location of the carbon-fiber stiffeners is indicated in the figure. The irregular discretization in the wing-tip region is chosen to allow for accurate modeling of the launcher-beam attachment.

Material properties were derived in several steps, starting by the glass-fiber plate without the carbon-fiber spars. Vibration testing of the plate was performed to obtain material data by matching the measured eigenfrequencies to the eigenfrequencies predicted by the numerical model. The wing was freely supported to exclude effects due to imperfections of the boundary conditions after it was mounted to the wind-tunnel floor.

Material data from the manufacturer were used to determine material properties of the carbon-fiber spars. Once attached to the glass-fiber wing, another vibration test was performed to validate the material data. After that, the wing was mounted into the wind tunnel, and yet another vibration test was performed. The measured eigenfrequencies appeared to be somewhat lower than expected for a rigidly clamped wing, and it was found that introducing some flexibility in the numerical model of the clamping improved the frequency matching. The flexibility was chosen such that the first and second eigenfrequencies predicted by the numerical model were within 0.1 Hz of the measured eigenfrequencies from the vibration testing.

The missile was assumed to be rigid, and only the mass properties of the missile were modeled. A grid point representing the degrees of freedom of the missile assembly was defined and attached to the wing tip. In the experimental setup, the missile launcher was rigidly

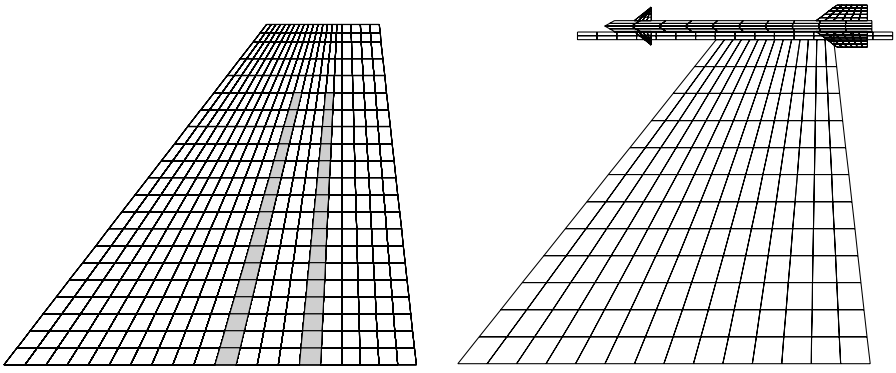

a) Structural elements b) Aerodynamic panels

Fig. 3 Discretization of the numerical model.

connected to the wing tip along the entire tip chord, thus eliminating chordwise bending deformations of the wing-tip region. Masses for the various components of the missile were then rigidly attached to that grid point.

The structural damping was neglected in the structural model, and it was assumed that this simplification results in slightly conservative flutter predictions without any significant impact on the general flutter behavior. The numerical approaches presented in the following sections are based on a model without structural damping, but could easily be modified to include damping.

Aerodynamic Modeling

The aerodynamic modeling was performed in both NASTRAN and ZAERO. NASTRAN `CAERO1` elements were used to model aerodynamic panels for computation of doublet-lattice [7] aerodynamic loads. The wing surface was covered by 12 spanwise times 14 chordwise lifting surfaces equally distributed on the wing area. The launcher beam and missile body were modeled as flat panels parallel to the wing surface, because it was assumed that in-plane aerodynamic loads produced by panels perpendicular to the wing surface can be neglected in the flutter analysis. Depending on the configuration, between 200 (configuration 5) and 402 (configuration 1) aerodynamic panels were defined. In Fig. 3b, the NASTRAN aerodynamic panels for the full missile configuration are shown.

The ZAERO aerodynamic model using `CAERO7` elements uses the same discretization as the NASTRAN model for the wing, the missile launcher beam, and the missile fins. The missile body, however, was modeled using `BODY7` elements.

To connect the structure and the aerodynamic panels, a surface spline was defined for the wing plate using `SPLINE1` in both NASTRAN and ZAERO, and a beam spline was defined for connecting the missile panels to the grid point defining the missile motion, using `SPLINE5` in NASTRAN and `ATTACH` in ZAERO.

Flutter Results

In most applications, flutter testing of real aircraft is restricted to subcritical airspeeds, due to the high risk involved in operating the aircraft in flutter conditions. As the airspeed approaches the flutter stability limit, the aeroelastic damping of the structure is reduced, leading to weakly damped oscillations after the wing is subject to external excitation. The oscillations correspond to complex eigenvalues in a linear stability analysis, in which the real and imaginary parts represent the damping and frequency of a particular mode, respectively. Rather than comparing the flutter speed from numerical predictions and experiments, eigenvalues can be compared instead to validate the numerical model without the need to operate the aircraft at the flutter limit. The wind-tunnel model, however, was designed to operate at, and even beyond, the flutter limit, and eigenvalues representing both stable and unstable conditions can be measured and compared with numerical predictions.

Experimental Results

Experiments were performed at different airspeeds and for different missile configurations. To estimate eigenvalues from oscillations, the wind-tunnel model was equipped with an accelerometer in the wing-tip region to monitor the structural response to an impulse excitation. Below the flutter limit, some beating was typically observed in the wave during the first couple of seconds, indicating the presence of several modes. This can hardly be avoided when using impulse excitation as in the present case, because many different modes will be excited simultaneously. However, as the other modes were significantly more damped, the critical mode quickly dominated the motion. Above the flutter limit, there was no need for external excitation, because any disturbance in the airflow can initiate the oscillations. Despite the wing being designed for large deflections, wind-tunnel testing above the flutter speed is dangerous, due to the steadily increasing amplitudes, and would eventually cause damage to the model.

Experiments were primarily performed at subcritical airspeeds, and only a few experiments were run above the flutter speed to ensure that the mode actually became unstable. From the measurements, complex experimental eigenvalues $p_{\text{exp}} = \sigma_{\text{exp}} + i\omega_{\text{exp}}$ were estimated by identifying a state-space system based on the measured time series. Frequency $f_{\text{exp}} = \omega_{\text{exp}}/(2\pi)$ and damping defined as $2\sigma_{\text{exp}}/\omega_{\text{exp}}$ are then extracted from the eigenvalues. Because the measured and predicted frequencies differed by less than 3% of the measured value in all cases, results for the damping are emphasized in the following.

The data were first collected for the most simple configuration without the missile attached to the wing. Figure 4a shows the resulting damping versus airspeed. The flutter speed was found to be between 25 and 26 m/s, where the damping crosses zero, corresponding to a purely imaginary eigenvalue. Similar experiments were performed for all configurations. Note that numerical predictions, which were obtained as described in the next section, are included in the figure.

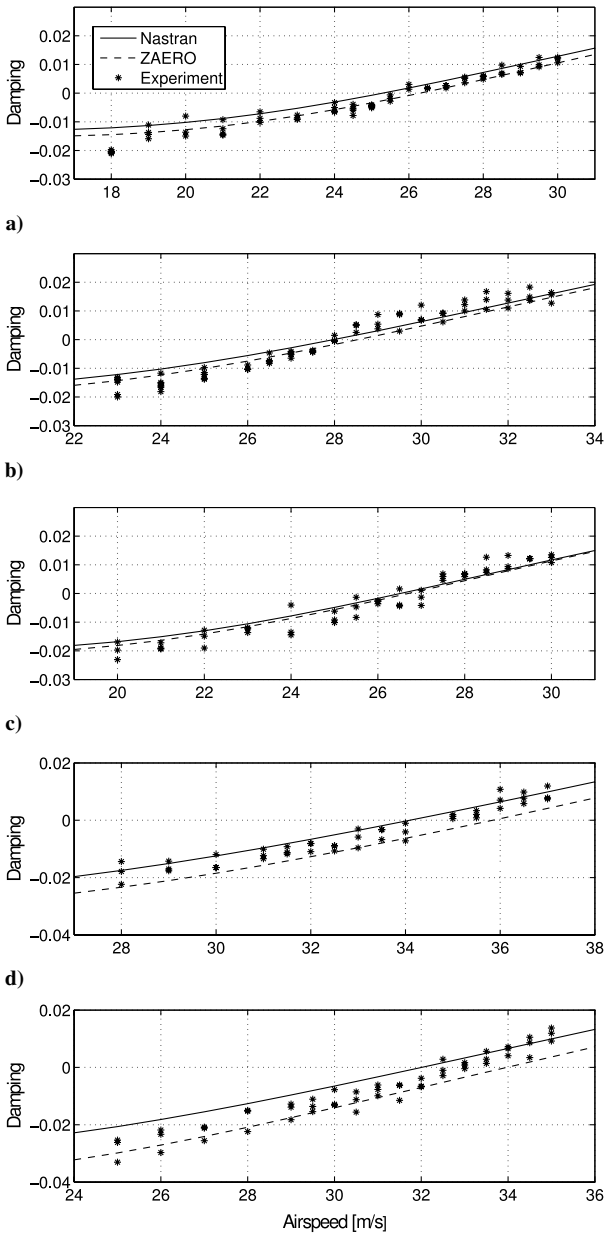

Fig. 4 Comparison of numerical and experimental results a) without the missile, b) with missile body attached, c) with missile body and canard fins, d) with missile body and rear fins, and e) with complete missile.

Nominal Flutter Analysis

The nominal analysis is performed by solving the flutter equation:

$$F_0(p)\eta = [M_0 p^2 + (L/V)^2 K_0 - (\rho L^2/2) Q_0(ik)]\eta = 0 \quad (1)$$

where M_0 and K_0 are the nominal mass and stiffness matrices, respectively; $Q_0(ik)$ is the nominal frequency-domain aerodynamic matrix; the airspeed and air density are denoted as V and ρ, respectively; and L is the reference length used to make the equation nondimensional. As the present study is limited to the low-speed regime, the dependence on the Mach number has been omitted for simplicity.

The flutter equation (1) is a nonlinear eigenvalue problem with complex eigenvalues $p = g + ik$ and corresponding eigenvectors of modal coordinates η. Specifically, the eigenvalues are the values of p that makes the flutter matrix $F_0(p)$ singular, such that $\det[F_0(p)] = 0$ holds. The imaginary part of the eigenvalue is the reduced frequency $k = \omega \cdot L/V$, and the real part $g = \sigma \cdot L/V$ is a measure of the damping of the system. As for the eigenvalues estimated by the experimental time series, the damping is then defined as $2g/k$. The flutter stability limit is found as the damping of some mode becomes zero. Note that ω and σ used in the analysis correspond to ω_{exp} and σ_{exp} from the experiment, respectively.

In this work, the nominal eigenvalues were computed using the modified p-k method in [8]. In Fig. 4a, the numerical results for the critical mode are shown along with the measurements. The comparison shows that the damping is predicted very well by the numerical model. Note that the experimental data are more noisy for lower velocities. This is due to the higher aeroelastic damping, making the oscillations decay faster, which leads to shorter sampling times and therefore less accurate values for the damping. It should be noted, however, that a discrepancy between the predicted and experimental results is expected, mainly because the aerodynamic model is based on linear potential flow, but also due to imperfections in the structural model. Consequently, increasing the number of aerodynamic panels to improve the accuracy of the potential flow model will not, in general, eliminate the gap between theory and experiments.

Influence of External Stores

When attaching the missile to the wing, the flutter behavior is expected to change both in the analysis and in the experiment. Because mass balancing was used to account for the missile components, however, all configurations should have similar structural properties, and the main differences are expected to be due to different aerodynamic loads. The missile was attached to the wing in several steps, beginning with the missile body (configuration 4). Flutter results for this configuration are shown in Fig. 4b. The figure shows that the quality of the damping data is somewhat lower than in the case before. Nevertheless, the damping values obtained in the experiments agree fairly well with the predictions. NASTRAN and ZAERO produce very similar results for this configuration.

In the next step, the canard fins were attached to the model. The damping curves for this configuration are shown in Fig. 4c. Compared with the case without canard fins, the flutter speed was reduced by 1.5 m/s in the analysis. There is some scatter in the measured damping, but it seems that the mean value fits reasonably well to the numerical results.

Next, the canard fins were removed again and the rear fins were attached to the missile. Results from these investigations are shown in Fig. 4d. The rear fins increase the flutter speed significantly, which is predicted by the analysis and also found in the experimental investigations. The NASTRAN and ZAERO damping predictions deviate slightly from each other, with the experimental values being located between these curves. NASTRAN is slightly conservative, whereas ZAERO overpredicts the flutter speed.

Finally, the complete configuration was considered by attaching the canard wings, with results as shown in Fig. 4e. As before, the canard wings lead to a destabilization of the wing. In the analysis, this can be seen by a reduction of the predicted flutter speed from 34 to 32 m/s for the NASTRAN model and from 36 to 34 m/s for ZAERO. The experiment is again between the predictions by NASTRAN and ZAERO, with NASTRAN being slightly conservative. There is also a more pronounced scatter in the experimental damping data.

The investigations of the different configurations show that the numerical model is fairly accurate. As the rear fins are included, the predictions by NASTRAN and ZAERO deviate from each other, with the experimental data being between the predictions. In the next section, aerodynamic modeling imperfections will be taken into account to derive robust flutter bounds that capture the experimental data entirely. Because of the similar behavior of the NASTRAN and the ZAERO models, the robust approach is based on the NASTRAN model only. It is assumed that a robust approach based on the ZAERO model would produce similar results.

Robust Approach

Comparison between the experimental and predicted eigenvalues indicates that the numerical model captures the flutter behavior fairly well. As the missile is attached to the wing, however, the analysis is not as accurate: in particular, as the rear fins are included. This sensitivity to geometric details of external stores has also been reported in other studies [9]. It is therefore assumed that the error is due to modeling imperfections that can be accounted for by introducing uncertainties in the numerical model. In the present case, the structural model has been tuned to fit experimental data from vibration-testing experiments and is considered to be accurate. Uncertainty is only introduced in the aerodynamic forces, in which the modeling approach described in [1,2] is used to allow for uncertainty in selected aerodynamic panels. Once the uncertainty description is developed, μ-p model validation and flutter analysis as described in [4] is applied to predict bounds on the flutter speed for increasing airspeed in the wind-tunnel test.

Uncertainty Modeling

Aerodynamic uncertainty is introduced such that the pressure coefficients for a patch (subset) of aerodynamic panels are allowed to vary in a uniform manner according to $c_p = (1 + w_j \delta_j) c_{p0}$, where c_{p0} are the nominal pressure coefficients, and $w_j > 0$ is a real-valued uncertainty bound that scales the complex-valued uncertainty parameter δ_j such that $|\delta_i| \leq 1$. Thus, a bound $w_j = 0.1$ means that the pressure coefficients in patch j are allowed to vary up to 10% in a uniform manner.

Introducing a set of patches on the lifting surface, the uncertain aerodynamic matrix can be written in the form

$$Q(ik, \delta) = Q_0(ik) + \sum_{j=1}^{n_p} w_j \delta_j Q_j(ik) \quad (2)$$

where $\delta \in D$ is the vector of uncertainty parameters that belongs to the set $D = \{\delta: \|\delta\|_\infty \leq 1\}$, n_p is the number of uncertain patches, and $Q_j(ik)$ are aerodynamic perturbation matrices that determine the influence of the different patches.

As the nominal and experimental results have shown, the aerodynamics of the missile assembly have substantial impact on the flutter behavior. The entire wing-tip region was therefore considered for the uncertainty modeling. As shown in Fig. 5, 20 different patches containing aerodynamic panels were defined for the full missile configuration. However, as described later, it was possible to use a subset of these patches in the robust analysis without compromising the accuracy.

Robust Eigenvalue Analysis

Instead of computing nominal eigenvalues from Eq. (1), the objective is to compute robust eigenvalues by considering the uncertain flutter equation:

$$F(p, \delta)\eta = [M_0 p^2 + (L/V)^2 K_0 - (\rho L^2/2) Q(ik, \delta)]\eta = 0 \quad (3)$$

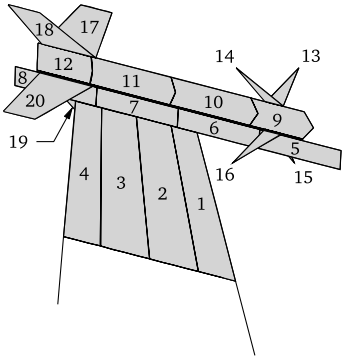

Fig. 5 Uncertain patches in the wing-tip region.

where the flutter matrix $F(p, \delta)$ now depends on the unknown but bounded parameters in $\delta \in D$ through the aerodynamic matrix $Q(ik, \delta)$ defined in Eq. (2). For $\delta = 0$, the equation reduces to Eq. (1) and each mode is represented by a single nominal eigenvalue. When the uncertainty is introduced, the nominal eigenvalue expands to a set (region) of feasible eigenvalues in the complex plane. If the set of feasible eigenvalues can be computed and is distinct (i.e., does not overlap with the eigenvalue set of another mode), damping and frequency bounds can be extracted for the corresponding mode. Further, if all eigenvalue sets are restricted to the left half-plane ($g < 0$), the system is robustly stable subject to the uncertainty.

In this work, robust eigenvalues for the critical mode were computed using the recently developed μ-p method [4]. When applied to the present problem, the μ-p method exploits structured singular value (or μ) analysis [10] to investigate if some uncertainty $\delta \in D$ can make the flutter determinant $\det[F(p, \delta)] = 0$ for a given value of p. If this is true, then p is an eigenvalue of Eq. (3) for some $\delta \in D$. Using this result, a search algorithm is applied in the complex plane to compute robust eigenvalues and extract damping bounds. The μ solver in MATLAB [11] was used for the μ-p analysis, using the default settings.

Model Validation

The μ-p framework can also be used to compute uncertainty bounds based on experimental estimates of flutter eigenvalues [4]. Assume that an eigenvalue $p_{\text{exp}} = g_{\text{exp}} + ik_{\text{exp}}$ has been obtained in flight testing. The basic principle of so-called p validation is to compute an uncertainty bound such that the uncertain flutter equation (3) has an eigenvalue $p = p_{\text{exp}}$ for some $\delta \in D$ (the experimental eigenvalue is matched). It is also possible to perform g validation to compute the minimum uncertainty bound such that Eq. (3) has an eigenvalue with $Re(p) = g_{\text{exp}}$ for some $\delta \in D$ (only the experimental damping is matched). The latter technique will result in a smaller uncertainty bound and is useful in cases when a discrepancy in frequency is known to be caused by a mechanism that is not captured by the uncertainty description (and has a modest influence on the damping).

In this study, the frequency offset was found to be rather weakly correlated to the damping offset for the different configurations. It was therefore decided to apply g validation to the critical mode to size and validate the aerodynamic uncertainty description. First, the sensitivity of the aeroelastic damping to aerodynamic uncertainty in the different patches was investigated by computing the minimum uncertainty bounds w_j required to match the experimental damping at $V = 25$ m/s in Fig. 4e (using only one patch at a time). The damping was found to be the most sensitive to uncertainty in patch 1, in which an uncertainty bound $w_1 = 0.49$ was required to match all experimental values. This means that if the uncertainty is restricted to the first patch only, a 49% aerodynamic perturbation in this region of the lifting surface is necessary to match the experimental data.

It was also found that the seven patches (1, 3, 4, 9, 12, 17, and 18) with the most significant impact are all located in a position in which they can effectively influence the aerodynamic twist moment in the wing tip, which appears to be the main source of uncertainty.

To obtain an uncertainty description of reasonable size (leading to a more efficient robust analysis), one possibility is to limit the uncertainty description to these patches only. Assuming an equal bound in each patch (other weightings w_i/w_j are possible) then results in the bounds $w_j = 0.18$ for all seven patches. If all 20 patches are included, the bounds $w_j = 0.13$ are required to validate the model. Note that the number of considered patches, as well as their layout and relative significance w_i/w_j, is somewhat arbitrary. However, as shown in the next section, the robust flutter bounds appears to be quite insensitive to these details as long as the main uncertainty mechanism is captured and model validation is performed.

Robust Flutter Analysis and Testing

Next, μ-p flutter analysis [4] was used to compute robust eigenvalues with minimum and maximum real part g for increasing airspeed. Robust analysis of the critical mode was performed for three different uncertainty descriptions, including 1) the most significant patch, 2) the seven most significant patches, and 3) all 20 patches. Regarding the required computational effort, the experience gained so far with the present type of uncertainty model (with only complex uncertainty parameters) is that it is comparable with that of the nominal analysis (thus, very modest).

Results from robust flutter analysis using the uncertainty bounds from g validation at 25 m/s are displayed in the damping graph of Fig. 6. Another observation is that the predicted worst- and best-case flutter speeds are almost the same for all uncertainty descriptions. In this graph, it can be observed that the predicted best-case damping perfectly matches the most deviating experimental value at 25 m/s, as should be the case using g validation. The models based on 7 and 20 patches produce almost identical results, but even the model based on one single patch is close. Based on this result, the model with seven patches was selected as the baseline for further analysis. Based on g validation at 25 m/s, the flutter speed was then predicted to be in the range of 28.2–35.8 m/s.

In a flight-testing scenario, the μ-p framework would be applied to obtain successive estimates of the robust flutter boundaries. Although the present case study is more simple, this procedure can still be demonstrated. Figure 7 shows the predicted bounds on the flutter speed for a successive update of the uncertainty bounds as the test speed in the wind tunnel is increased. Note that the nominally predicted flutter speed is 32 m/s and is independent of any uncertainty in the model. At 25 m/s, the predicted range of 28.2–35.8 m/s from Fig. 6 is displayed. As the test speed is increased and successive model validations are performed, the quality of the robust flutter bounds is successively improved.

The lower-bound flutter speed is reached at about 30 m/s in the test. Above this speed, robust stability is no longer guaranteed. However, because the nominal model consistently predicts a too-low damping, the experimental flutter speed is expected to be higher than the nominal flutter speed. In this case, the quality of the robust

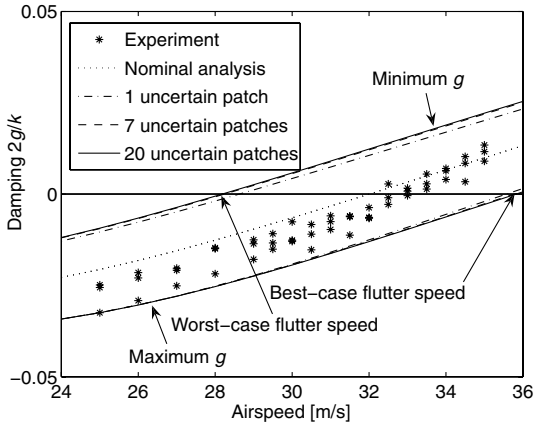

Fig. 6 Damping graph from robust analysis based on model validation at $V = 25$ m/s.

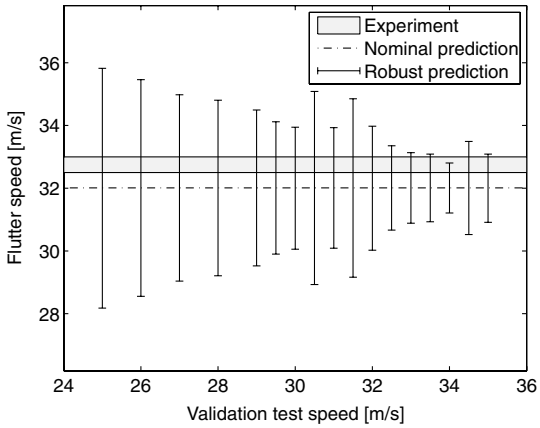

Fig. 7 Robust flutter speeds based on successive model validation.

analysis should therefore be judged in terms of the closeness between the upper-bound flutter speed and the true flutter speed. If the flutter speed is taken to be 32.5 m/s (where instability could first be detected in the test), the upper-bound flutter speed differs by less than 1 m/s from this value at the test speed of 32.5 m/s (see Fig. 7). Consequently, the procedure based on successive g validation and μ-p flutter analysis produced very accurate results in this case. It may finally be noted that even test speeds above the flutter speed (hence unstable test points) produced reliable bounds on the flutter speed.

Conclusions

The present study has demonstrated the capability of μ-p flutter analysis to produce reliable bounds on the flutter speed in the presence of uncertain external-store aerodynamics. A generic delta-wing configuration with a wing-tip external store was considered for the flutter investigations. An aerodynamic uncertainty description was developed based on results from a series of wind-tunnel tests and flutter analyses of different external-store configurations. A simple but very useful approach to size the aerodynamic uncertainty description was presented, in which a μ-p model validation technique was used to perform a sensitivity analysis of each aerodynamic patch on the lifting surface. The result of the sensitivity analysis could also be used to identify the main source of uncertainty, which appeared in this case to be the aerodynamic twist moment in the wing tip. Finally, it was found that the computed bounds on the flutter speed were quite insensitive to details in the aerodynamic uncertainty description as long as model validation against experimental data was performed.

Acknowledgment

This research was financially supported by the Swedish Aeronautics Research Program project S4303.

References

[1] Borglund, D., "The μ-k Method for Robust Flutter Solutions," *Journal of Aircraft*, Vol. 41, No. 5, 2004, pp. 1209–1216. doi:10.2514/1.3062

[2] Borglund, D., and Ringertz, U., "Efficient Computation of Robust Flutter Boundaries Using the μ-k Method," *Journal of Aircraft*, Vol. 43, No. 6, 2006, pp. 1763–1769. doi:10.2514/1.20190

[3] Moulin, B., "Modeling of Aeroservoelastic Systems with Structural and Aerodynamic Variations," *AIAA Journal*, Vol. 43, No. 12, 2005, pp. 2503–2513. doi:10.2514/1.15023

[4] Borglund, D., "Robust Eigenvalue Analysis Using the Structured Singular Value: The μ-p Flutter Method," *AIAA Journal*, Vol. 46, No. 11, 2008, pp. 2806–2813. doi:10.2514/1.35859

[5] NASTRAN, Software Package, Ver. 2005, MSC Software Corp., Santa Ana, CA, 2005.

[6] ZAERO, Software Package, Ver. 7.1, Zona Technology, Scottsdale, AZ, 2004.

[7] Albano, E., and Rodden, W. P., "A Doublet-Lattice Method for Calculating Lift Distributions on Oscillating Surfaces in Subsonic Flows," *AIAA Journal*, Vol. 7, No. 2, 1969, pp. 279–285. doi:10.2514/3.5086

[8] Bäck, P., and Ringertz, U., "Convergence of Methods for Nonlinear Eigenvalue Problems," *AIAA Journal*, Vol. 35, No. 6, 1997, pp. 1084–1087. doi:10.2514/2.200

[9] Chen, P. C., Sarhaddi, D., and Liu, D. D., "Limit-Cycle Oscillation Studies of a Fighter with External Stores," AIAA Paper 98-1727, 1998.

[10] Zhou, K., Doyle, J. C., and Glover, K., *Robust and Optimal Control*, Prentice–Hall, Upper Saddle River, NJ, 1996, Chap. 11.

[11] MATLAB, Software Package, Ver. 7.4, The MathWorks, Inc., Natick, MA, 2007.